Biaxial testing of fibre-reinforced composite laminates

D V Hemelrijck[1*], **A Makris**[1], **C Ramault**[1], **E Lamkanfi**[2], **W V Paepegem**[2], and **D Lecompte**[3]
[1]Department of Mechanics of Materials and Constructions, Vrije Universiteit Brussel, Brussels, Belgium
[2]Department of Mechanical Construction and Production, Ghent University, Ghent, Belgium
[3]Royal Military Academy, Department of Civil and Materials Engineering, Brussels, Belgium

The manuscript was received on 4 February 2008 and was accepted after revision for publication on 4 July 2008.

DOI: 10.1243/14644207JMDA199

Abstract: Advanced composite material systems are increasingly used in almost every industrial branch. The structural components manufactured from these composite material systems are usually subjected to complex loading that leads to multi-axial stress and strain fields at critical surface locations. The current practice of using solely uniaxial test data to validate proposed material models is wholly inadequate. In order to test closer to reality, a biaxial test bench using four servo-hydraulic actuators with four load cells was developed. Besides the development of the test facility, a mixed numerical/experimental method was developed to determine the in-plane stiffness parameters from testing a single cruciform test specimen. To obtain the strength data an optimized geometry for the cruciform type specimen was designed. For the optimization procedure a full three-dimensional finite element model was used. The numerical results were validated with strain gauge, digital image correlation, and electronic speckle pattern interferometry data. The material system used for the experimental validation was glass fibre-reinforced epoxy with a lay-up $[(+45^\circ\ -45^\circ\ 0^\circ)_4(+45^\circ\ -45^\circ)]$ typically used for wind turbine blades.

Q1

Keywords: composites, biaxial loading, mechanical characterization

1 INTRODUCTION

Advanced composite material systems are increasingly used in almost every industrial branch. Besides applications in the automotive, aeronautical and sports sectors, there are numerous and ever-increasing industrial uses, including in: wind turbines, storage tanks, high-speed and precision machinery, gas turbine engines, and medical diagnostic equipment. Indeed, their outstanding mechanical performance added to their low weight and other unique and tailorable physical properties make composites the material system of first choice for many applications. The constituent parts of the structural components manufactured from these composite material systems are usually subjected to complex loading that leads to multi-axial stress and strain fields at critical surface locations. Consequently, a reliable design procedure validated rigorously by multi-axial experimental data is mandatory in order to ensure satisfactory performance over the predefined service period, and to avoid the use of excessive safety factors to cover the high level of uncertainty. In fact, the further growth of the use of advanced composite materials for structural applications will largely depend on the ability to model and simulate the behaviour of these materials successfully. Numerous theories have been proposed to predict the response of composite materials but, in order to apply these analysis tools for structural design, experimental validation under a variety of complex loading conditions is mandatory. As composite materials generate complex biaxial and multi-axial stress states [**1**], even for simple uniaxial loading, the current practice of using solely uniaxial test data is wholly inadequate and consequently, testing closer to reality is of paramount importance.

Furthermore, as a result of the First World Wide Failure Exercise (WWFE) [**2**], it became clear that none of the 19 evaluated failure theories worked well for all the 14 test cases. It also demonstrated the huge lack of reliable experimental data. Indeed, during the last decade the composite testing community has successfully developed the ability to characterize

Corresponding author: Department of Mechanics of Materials and Constructions, Vrije Universiteit Brussel, Pleinlaan 2, Brussels 1050, Belgium. email: dvhemelr@vub.ac.be

accurately the uniaxial response of fibre-reinforced composite materials. Several standardized test methods have been developed to evaluate the in-plane shear, the axial and transverse tensile, and the axial and transverse compressive response. Unfortunately, test methods to determine the same properties under complex stress states did not make the same progress. The non-homogeneous and strong anisotropic response of composite materials and the fact that such complex experiments demand expensive and sophisticated test equipment are certainly the main reasons why multi-axial (biaxial or triaxial) test methods have not obtained the same level of maturity, and also possible explanations of why there is so little existing capability available to evaluate the multi-axial response of composite materials [**3**–**5**]. Nevertheless, different techniques with varying complexity have been developed for producing biaxial stress states over the past decades. These techniques may be classified into two categories [**6**]: (a) tests using a single loading system and (b) tests using two or more independent loading systems. In the first category, the biaxial stress ratio depends on the specimen's geometry or on the loading fixture configuration, whereas in the second category it is specified by the applied load magnitude. Examples of the first category include bending tests on cantilever beams, anticlastic bending tests of rhomboidal or rectangular shaped composite plates, bulge tests, equibiaxial loading of disc-shaped specimens, and tests on cruciform specimens with a spatial pantograph. Examples of the second category are round bars under bending-torsion, thin-wall tubes subjected to a combination of axial loading and torsion or internal/external pressure, and cruciform specimens under in-plane biaxial loading. The technique with the thin-wall tube is the most popular, [**7**] and seems to be very versatile, because it allows tests with any constant load ratio to be performed. However, it also presents some inconveniences [**6**, **8**, **9**] as for instance: (a) the radial stress gradients, depending on the thickness of the tube, and the applied load, may not be negligible; (b) real construction components in fibre-reinforced composite materials are often flat or gently curved and differ much from tubular specimens; (c) thin walled tubes are not easy to fabricate; (d) obtaining a perfect alignment and load introduction is not straightforward; (f) thin tubular specimens can experience various forms of elastic instability when they are subjected to circumferential or axial compression or torsion loads; and (g) tubes may exhibit changes in geometry during loading, but these effects are usually ignored when processing experimental results.

Consequently, to our knowledge, the most appropriate method for testing sheet materials consists of applying axial forces to the loading arms of a cruciform type specimen. Such a system using servo-hydraulic actuators was developed at the Department of Mechanics of Materials and Construction (MeMC) of the Free University of Brussels (VUB) [**10**]. Another challenge, besides the development of the test facility was the design and optimization of the geometry of the cruciform type specimen for stiffness as well as strength characterization of fibre-reinforced composite laminates [**11**–**13**]. The results related to this study are included in the present paper. Also included is a small overview of the test facility. For a full detailed report please read reference [**10**].

2 PLANE BIAXIAL TEST BENCH FOR CRUCIFORM TEST SPECIMENS

The biaxial test rig, Fig. 1, developed at the VUB, has a capacity of 100 kN in each perpendicular direction, but only in tension, limiting the experimental results to the first quadrant of the two-dimensional stress space. Since cylinders without hydrostatic bearings are used, failure or slip in one arm of the specimen will result in sudden radial forces, which could seriously damage the servo-hydraulic cylinders and load cells. To prevent this, hinges were used to connect the specimen to the load cells and the servo-hydraulic cylinders to the test frame. Using four hinges in each loading direction results in an unstable situation in compression and consequently only tension loads can be applied. The stroke of the cylinders is 150 mm. The loading may be static or dynamic up to a frequency of 20 Hz. Each cylinder is independently controlled and any type of loading waveform, including spectral sequences of variable amplitude, can be efficiently introduced using the dedicated software and control system.

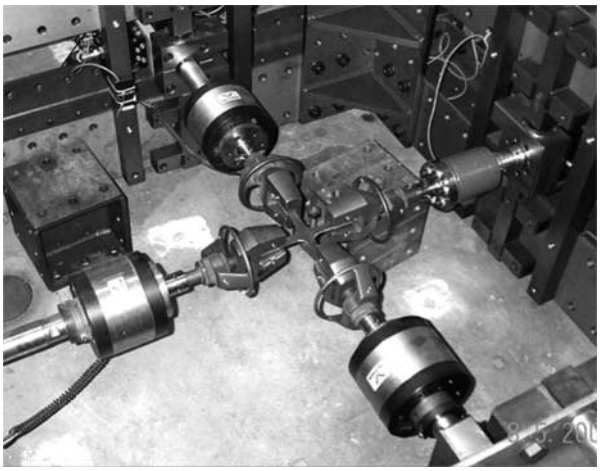

Fig. 1 Biaxial test bench

3 STIFFNESS CHARACTERIZATION VIA THE USE OF AN INVERSE METHOD

3.1 Introduction

Stiffness characterization using uniaxial test procedures is straightforward: the initial cross-section of the specimen is measured, during loading s the load is monitored using a calibrated load cell, and the axial and transverse strain, using an extensometer or strain gauge. The load divided by the initial cross-section yields the stress and consequently the stress–strain curve can be plotted from which the stiffness modulus, say E_1 (fibre direction), can be determined. To determine E_2, the stiffness modulus in the transverse direction, a similar procedure is followed. For the evaluation of the shear properties a $\pm 45^\circ$ off-axis or Iosipescu type specimen is used. Obviously, for full stiffness characterization of a composite laminate several tests are needed. It will be demonstrated that these tests can be replaced by a single biaxial test of a cruciform type specimen. In order to do so a mixed numerical experimental technique, integrating a full-field measurement technique, a finite-element method, and an optimization procedure, was developed in cooperation with the Royal Military Academy (RMA) [**14**, **15**]. In the present paper, a method is proposed for the identification of the in-plane engineering constants $E1$, $E2$, $G12$, and $\nu 12$ of an orthotropic material based on surface measurements. The responses of the system, i.e. the surface displacements, are measured with digital image correlation (DIC). Strains are subsequently calculated. A finite element model of the cruciform specimen serves as numerical counterpart for the experimental set-up. The difference between the experimental and numerical strains (the cost function) is minimized in a least squares sense by updating the values of the engineering constants. The optimization of the parameters is performed by the Gauss–Newton method. In contrast to a direct problem, which is the classical problem where a given experiment is simulated in order to obtain the stresses and the strains, inverse problems are concerned with the determination of the unknown state of a mechanical system, using information gathered from the response to stimuli on the system [**16**]. Not only is the boundary information used, but also, relevant information obtained from full-field surface measurements is integrated. The inverse method described here can be narrowed to parameter identification, as the only item of interest is the determination of the constitutive parameters. The values of these parameters cannot be derived immediately from the experiment due to the specimen geometry. A numerical analysis is necessary to simulate the experiment. However, this requires that the material parameters are known. The identification problem can be formulated as an optimization problem where the function to be minimized is an error function that expresses the difference between numerical simulation and experimental results. In the present case the strains are used as output data. Figure 2 represents the flow chart of the inverse modeling problem.

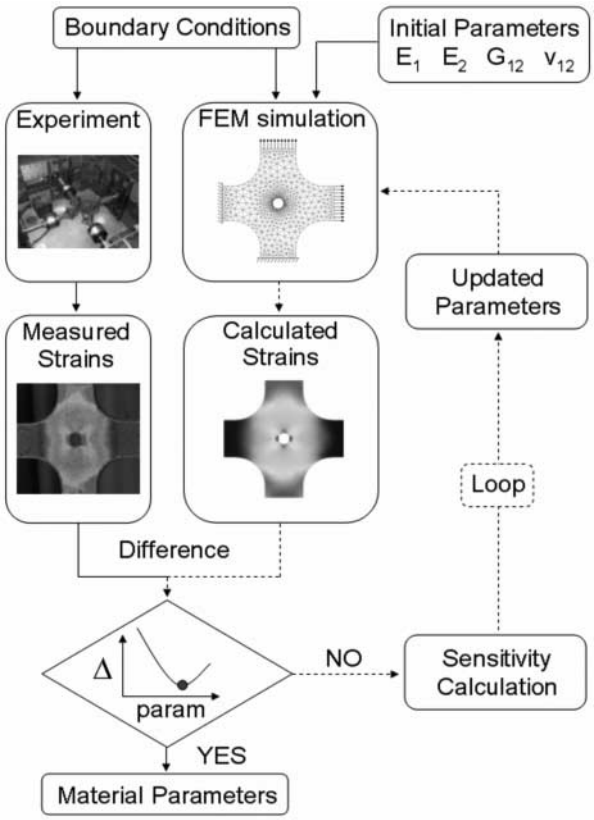

Fig. 2 Flow chart of determination process

3.2 Optimization algorithm

The optimization of the apparent engineering constants is performed by the Gauss–Newton method. The cost function that is minimized is a simple least squares formulation. Expression (1) shows the form of the least-squares cost function that is minimized. The residuals in the function are formed by the differences between the experimental and the numerical strains

$$C(\boldsymbol{p}) = C(\boldsymbol{\varepsilon}(\boldsymbol{p}), \boldsymbol{p}) = \sqrt{\sum_{i=1}^{n} \left[\frac{\boldsymbol{\varepsilon}_i^{\text{num}}(\boldsymbol{p}) - \boldsymbol{\varepsilon}_i^{\text{exp}}}{\boldsymbol{\varepsilon}_i^{\text{exp}}} \right]^2} \qquad (1)$$

The necessary condition for a cost function to attain its minimum is expressed by equation (2). The partial derivative of the function with respect to the different material parameters has to be zero. By developing a Taylor expansion of the numerical finite element strains around a given parameter set, an expression is obtained in which the difference between the

present parameters and their new estimates is given by equation (3)

$$\frac{\partial C(\boldsymbol{p})}{\partial p_i} = \frac{1}{C(\boldsymbol{p})} \sum_{j=1}^{n} \left[\frac{\boldsymbol{\varepsilon}_i^{\text{num}}(\boldsymbol{p}) - \boldsymbol{\varepsilon}_i^{\text{exp}}}{\boldsymbol{\varepsilon}_i^{\text{exp}}} \right] \frac{\partial \boldsymbol{\varepsilon}_j^{\text{num}}}{\partial \boldsymbol{p}_i} = 0 \quad (2)$$

$$\varepsilon_i^{\text{num}}(\boldsymbol{p}) \cong \boldsymbol{\varepsilon}_i^{\text{num}}(\boldsymbol{p}^k) + \sum_{j=1}^{m} \frac{\partial \boldsymbol{\varepsilon}_i^{\text{num}}(\boldsymbol{p}^k)}{\partial \boldsymbol{p}_j} \left(\boldsymbol{p}_j - \boldsymbol{p}_j^k \right) \quad (3)$$

Substituting equation (3) in equation (2) and rearranging some terms, yields equation (4), and the parameter updates are obtained.

$$\Delta \boldsymbol{p} = \left(\mathbf{S}^t \mathbf{S} \right)^{-1} \mathbf{S}^t \left[\boldsymbol{\varepsilon}^{\text{exp}} - \boldsymbol{\varepsilon}^{\text{num}}(\boldsymbol{p}^k) \right] \quad (4)$$

where $\Delta \boldsymbol{p}$ is the column vector of the parameter updates of E_1, E_2, G_{12}, and ν_{12}, $\boldsymbol{\varepsilon}^{\text{exp}}$ the column vector of the experimental strains, $\boldsymbol{\varepsilon}^{\text{num}}(\boldsymbol{p}^k)$ the column vector of the finite element strains as a function of the four parameters at iteration k, and $\mathbf{S}^t$ the sensitivity matrix.

3.3 Sensitivity calculation

The sensitivity matrix (5) groups the sensitivity coefficients of the strain components in every element of the finite element mesh with respect to the elastic material parameters. The index n in equation (5) stands for the total number of elements. The components of this sensitivity matrix can be derived analytically from the constitutive relation between stress and strain, which is given by expression (6) in the case of a plane stress problem. The stresses that are used in the calculation of the derivatives are taken from the converged simulation in the actual iteration step. The values of the parameters are taken from the previous iteration step

$$\mathbf{S} = \begin{bmatrix} \frac{\partial \varepsilon_x^1}{\partial E_1} & \frac{\partial \varepsilon_x^1}{\partial E_2} & \frac{\partial \varepsilon_x^1}{\partial G_{12}} & \frac{\partial \varepsilon_x^1}{\partial \nu_{12}} \\ \frac{\partial \varepsilon_y^1}{\partial E_1} & \frac{\partial \varepsilon_y^1}{\partial E_2} & \frac{\partial \varepsilon_y^1}{\partial G_{12}} & \frac{\partial \varepsilon_y^1}{\partial \nu_{12}} \\ \frac{\partial \gamma_{xy}^1}{\partial E_1} & \frac{\partial \gamma_{xy}^1}{\partial E_2} & \frac{\partial \gamma_{xy}^1}{\partial G_{12}} & \frac{\partial \gamma_{xy}^1}{\partial \nu_{12}} \\ \vdots & \vdots & \vdots & \vdots \\ \frac{\partial \varepsilon_x^n}{\partial E_1} & \frac{\partial \varepsilon_x^n}{\partial E_2} & \frac{\partial \varepsilon_x^n}{\partial G_{12}} & \frac{\partial \varepsilon_x^n}{\partial \nu_{12}} \\ \frac{\partial \varepsilon_y^n}{\partial E_1} & \frac{\partial \varepsilon_y^n}{\partial E_2} & \frac{\partial \varepsilon_y^n}{\partial G_{12}} & \frac{\partial \varepsilon_y^n}{\partial \nu_{12}} \\ \frac{\partial \gamma_{xy}^n}{\partial E_1} & \frac{\partial \gamma_{xy}^n}{\partial E_2} & \frac{\partial \gamma_{xy}^n}{\partial G_{12}} & \frac{\partial \gamma_{xy}^n}{\partial \nu_{12}} \end{bmatrix} \quad (5)$$

$$\begin{Bmatrix} \varepsilon_x \\ \varepsilon_y \\ \gamma_{xy} \end{Bmatrix} = \begin{bmatrix} \frac{1}{E_1} & -\frac{\nu_{12}}{E_1} & 0 \\ -\frac{\nu_{12}}{E_1} & \frac{1}{E_2} & 0 \\ 0 & 0 & \frac{1}{G_{12}} \end{bmatrix} \begin{Bmatrix} \sigma_x \\ \sigma_y \\ \tau_{xy} \end{Bmatrix} \quad (6)$$

3.4 Experimental results

3.4.1 Tests on rectangular specimen

An extended database of experimental static and fatigue results on beamlike glass fibre-reinforced epoxy specimens with a $[(+45^\circ\ -45^\circ\ 0^\circ)_3(+45^\circ\ -45^\circ)]$-lay-up has been setup within the framework of the Optimat Blades project [**17**]. For the glass fibre-reinforced composite laminate with the mentioned lay-up, the average and standard deviation material parameter results of about 400 traditional beamlike tests are given in Table 1. E_1, E_2, and ν_{12} are obtained from static tensile tests while G_{12} is obtained from V-notch tests.

3.4.2 Tests on cruciform specimen (engineering constants)

For the identification of four independent elastic orthotropic parameters, a perforated and a non-perforated specimen are used. The reason for testing a specimen with a hole is to influence the overall deformation field and to make the measured strain fields more sensitive to the different material parameters. Since an experimentally obtained strain field is being dealt with here, this can be important. The specimens are subjected to three different ratios of biaxial tensile loads: 2.56/1, 3.85/1, and 5.77/1. Five successive load steps are imposed per ratio, so this means that 15 independently measured strain field triplets are available per specimen for the identification process. The same loads are used in the finite element simulation. A plane stress model is used with a uniformly distributed load as boundary condition. The convergence criterion used in the optimization phase ends the iteration process when the relative value of the parameter updates is inferior to 0.01 per cent. In all the optimization runs, the convergence criterion is reached in less than 13 iterations. The results of the identification process are shown in Tables 2 and 3 for both perforated and non-perforated specimens, in terms of the mean

Table 1 Material properties of the laminate obtained on beamlike specimens

	E_1 (GPa)	E_2 (GPa)	G_{12} (GPa)	ν_{12}
Average	27.03	14.21	8.1	0.455
Standard deviation (%)	4.4	6	9.5	9.2

Table 2 Material properties of perforated cruciform specimen

	E_1 (GPa)	E_2 (GPa)	G_{12} (GPa)	ν_{12}
Starting values	15	10	10	0.3
Average	25.11	12.17	7.05	0.483
Standard deviation (%)	5.4	6.8	8.9	7.7

Table 3 Material properties of non-perforated cruciform specimen

	E_1 (GPa)	E_2 (GPa)	G_{12} (GPa)	ν_{12}
Starting values	15	10	10	0.3
Average	25.11	13.31	7.69	0.467
Standard deviation (%)	2.8	6	6.8	6.6

parameter value and its corresponding standard deviation. They are obtained based on the 15 imposed load steps considered per specimen. The starting values for each of the parameters are mentioned as well. It can be observed that the difference between the results for both specimen types is reasonably small. The stability of the results obtained with the non-perforated specimen is slightly larger. This is probably due to the fact that the strain field is less complex and therefore easier to measure with the DIC technique than in the case of the perforated specimen.

4 STRENGTH PROPERTIES OF BIAXIALLY LOADED CRUCIFORM IN TENSION

Ideally, the same specimen geometry should be used for stiffness and strength characterization. Unfortunately, it was found that for the laminate stacking studied $[(+45^\circ\ -45^\circ\ 0^\circ)_3(+45^\circ\ -45^\circ)]$ too much load was transferred from one loading arm to the adjacent one. Consequently, the biaxial area in the central part of the specimen was not highly stressed and often premature failure occurred in the uniaxially loaded arms instead of the biaxially loaded central area. It is because of these experiences that the authors decided to put effort into developing and validating an optimized cruciform geometry for strength determination.

Another problem faced was stress calculation. The determination of the applied stress is straightforward for uniaxially loaded test coupons. For biaxially loaded cruciform-type specimens, where the exact loaded area is unknown, this is not the case. To define the stress, two different techniques are presented, one based on uniaxial strength data, and the other based on the constitutive law and the strain measurements.

4.1 Design of a cruciform test specimen

It has proved extremely difficult to develop a cruciform test specimen that fulfils simultaneously the following conditions: (a) there has to be a uniform stress/strain state in the biaxially loaded test zone; (b) failure has to occur in the biaxially loaded test zone and not in the uniaxially loaded arms; and (c) the results should be repeatable [**18**]. To optimize, the geometry finite element simulations were performed. The following parameters were investigated: (a) the rounding radius at the intersection of two arms; (b) the thickness of the biaxially loaded test zone in relation to the thickness of the arms; and (c) the shape of the test zone. Some selected geometries were also tested experimentally. Based on this preliminary study, of which the results are fully published in a previous paper [**10**] an optimized design of the cruciform specimen was proposed.

Currently, a more detailed three-dimensional finite element analysis is done to study the effect of geometric discontinuities on the stress and strain field. This is not possible with the shell model, because the shell elements do not allow for a correct modelling of the milled central area of the cruciform. Therefore a three-dimensional mesh of solid elements is generated, with one element per layer through the thickness. Every layer of composite material is assigned the elastic properties of the single lamina and the correct fibre orientation angle.

The experimental validation of the obtained numerical results was done using different experimental techniques. Strain gauges, DIC, and electronic speckle pattern interferometry (ESPI) were used to obtain the strain distribution, which was afterwards compared with three-dimensional finite element results (Fig. 3). Strain distribution and concentrations were also investigated in order to obtain an optimal geometry of the specimen. Five strain gauges were placed on the edge of the milled surface and one in the middle of the specimen in order to measure the longitudinal strain (Table 4). The uniformity of the strain field on the zone of interest was validated. Correlation among the three different measurement techniques and the finite-element method was very good (quantitative and qualitative) as the difference in strain results was limited to a small percentage.

Full field experimental techniques that enable the assessment of the overall strain distribution in the cruciform specimen are absolutely necessary. Strain measurements using a strain gauge or extensometer are not sufficient because both give an average value of the deformation along their gauge length and sometimes fail earlier than the specimen. To be able to study the symmetry of the strains and the occurring shear strains experimentally, a full field strain method is necessary. DIC is an experimental technique that offers

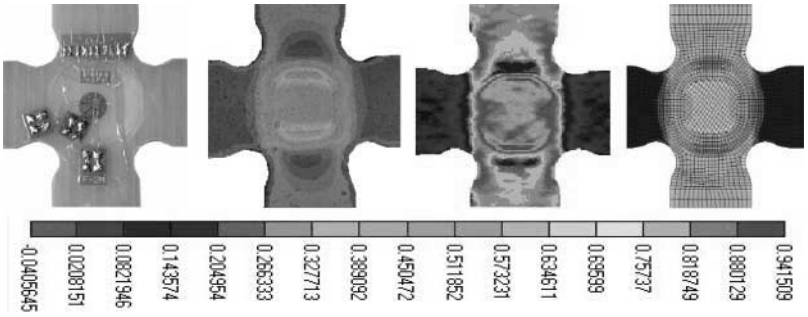

Fig. 3 Cruciform specimen showing the position of the strain gauges and the first principal strain fields from DIC, ESPI, and FEM, respectively for uniaxial tensional load (43 per cent of total failure load)

Table 4 Strain results for the five edge and the central strain gauges

	ε_1	ε_2	ε_3	ε_4	ε_5	$\varepsilon_{\text{central}}$
Longitudinal strain (%)	0.96	0.96	0.9	0.96	0.96	0.84

the possibility of determining displacement and deformation fields at the surface of objects under any kind of loading, based on a comparison between images taken at different load steps. The software processes and visualizes the data gathered in order to obtain an impression of the distribution of strains. A measurement session consists of taking several pictures of the region of interest (ROI) with a charge-coupled device (CCD) camera. In this case (Fig. 4), two cameras were used to be able to measure both in-plane and out of plane displacements on specimens not entirely flat as is the case for the specimens with a milled surface in the centre. Each picture corresponds to a different loading step. The camera uses a small rectangular piece of silicon that has been segmented into an array of 1392 by 1040 individual light-sensitive cells (pixels). Every pixel stores a certain grey scale value ranging from 0 to 4095, in agreement with the intensity of the light reflected by the surface of the tested specimen. ESPI is widely used in non-destructive testing (NDT), the deformations are made visible as fringe patterns while an inspected sample is loaded. Figure 5 shows the set-up of a uniaxial experiment on a cruciform specimen using both ESPI and DIC for validation of the displacement/strain results.

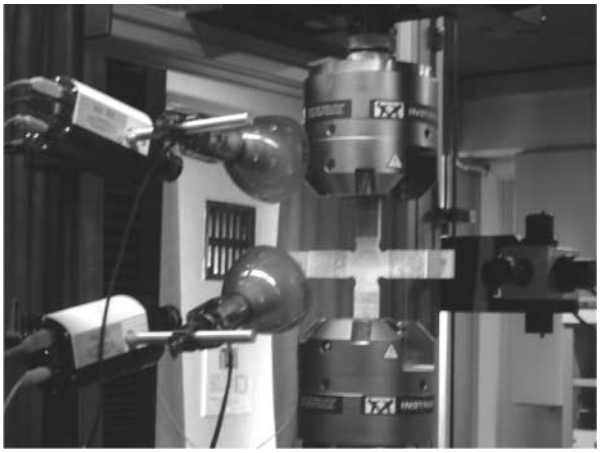

Fig. 5 DIC and ESPI techniques set-up

4.2 Stress calculations

4.2.1 Stress calculated from area

For uniaxial tension/compression tests, the determination of the applied stress is straightforward as the load and the area transferring the load can be measured. In the case of biaxial tests of the cruciform type specimens, only the applied load can be measured and the area is unknown. However, if the failure stress is assumed to be the same in a uniaxial test and a biaxial test of a cruciform loaded in one direction only, an equivalent area can be specified. The method is summarized in Fig. 6.

Two uniaxial tests on beam specimens and two uniaxial tests on cruciform specimens are needed to

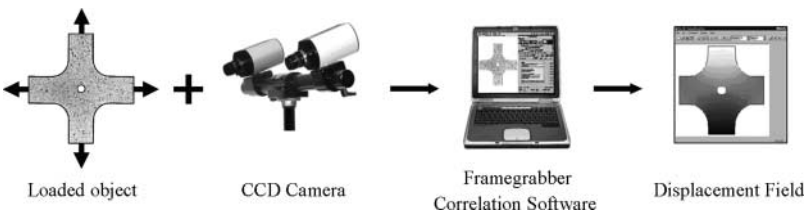

Fig. 4 Digital image correlation system

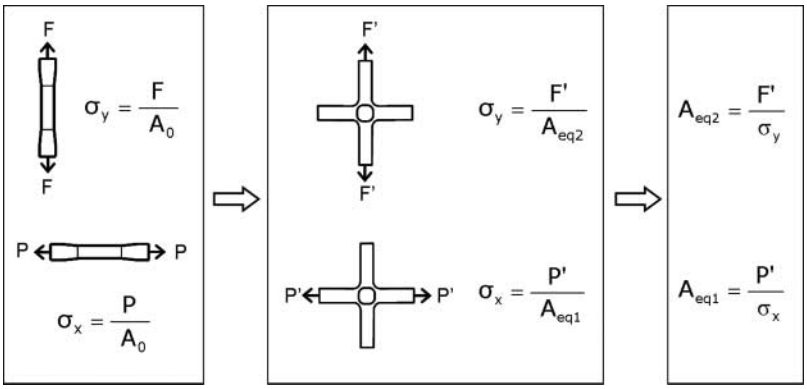

Fig. 6 Stress calculation method using equivalent area

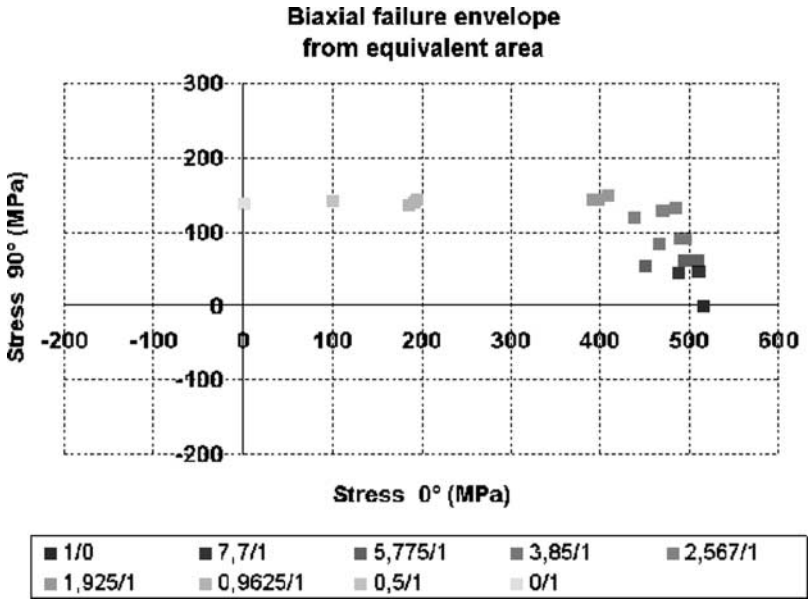

Fig. 7 Tension/tension failure stresses calculated using equivalent area

calculate the equivalent area A_{eq1} and A_{eq2} (which is loaded during a biaxial test) along the 0° fibres and transverse to them, respectively. From the four tests outputs the failure loads for each situation are known, furthermore, for the beam specimens the section A_0 is also known. For a different load ratio (load in 0°/load in 90°), the failure stresses of a biaxially loaded cruciform specimen could be calculated using the new failure loads divided by the equivalent area. Figure 7 shows the tension/tension failure envelope when the stresses are calculated from the equivalent area.

4.2.2 Stress calculated from constitutive law

In order to calculate stresses on a cruciform specimen with this method, strains that are measured by full field optical techniques (DIC and ESPI) are used. The strain vector is multiplied by the stiffness matrix to obtain the stress vector. All the elements of the stiffness matrix could be calculated using classical laminate theory or an inverse method [**14**, **15**]. The method is summarized in Fig. 8.

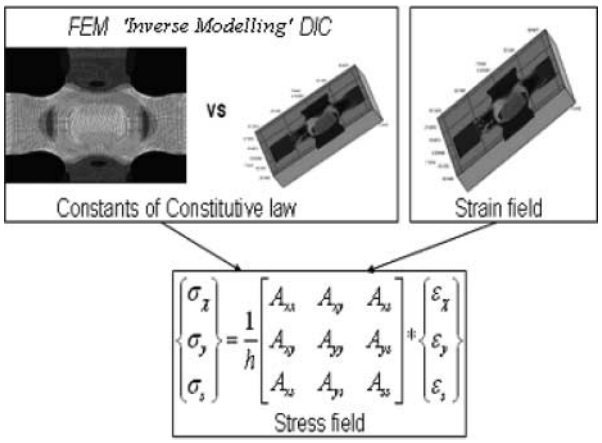

Fig. 8 Stress calculation method using strain measurements

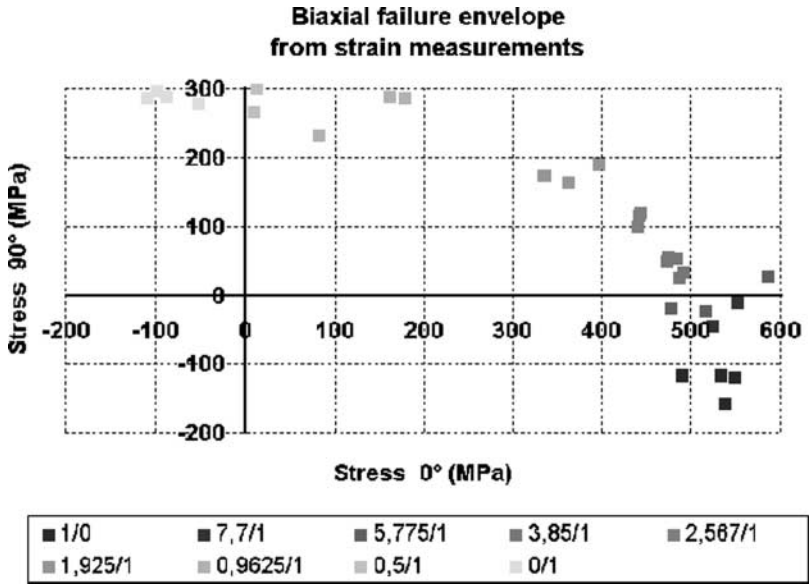

Fig. 9 Tension/tension failure stresses calculated using strain measurements

The method has some inconveniences as stresses are calculated using linear elastic constants. The response of the material $[(+45^\circ\ -45^\circ\ 0^\circ)_4(+45^\circ\ -45^\circ)]$ when it is tensioned along the fibre direction is almost linear, but is totally non-linear transverse to the fibre direction. The strength of the material due to this inconvenience is overestimated. Figure 9 shows the tension/tension failure envelope when the stresses are calculated from the material properties and the strain vector.

5 CONCLUSIONS

The combination of finite element simulations and experiments performed on different cruciform geometry types using the digital image correlation technique for full field strain measurements, led to the selection of a suitable geometry for biaxial testing of fibre-reinforced composite laminates. This geometry has a reduced thickness in the central region of the specimen, in combination with a fillet corner between two arms inside the material. These features cause failure to occur in the biaxially loaded test zone, rather than in the uniaxially loaded arms, giving failure strains comparable to strains obtained on beamlike specimens for the uniaxial load ratios. The digital image correlation technique used for full field strain measurements offers significant advantages over conventional techniques such as strain gauges. The spatially resolved strains led to a better understanding of the behaviour of composites under biaxial loads. The strain values obtained with the digital image correlation technique are comparable to those calculated in the finite element simulations. Using the proposed geometry strength, data was obtained for different load ratios. An inverse method has been proposed to determine the elastic parameters (E_1, E_2, G_{12}, and ν_{12}) of a glass fibre-reinforced epoxy with a $[(+45^\circ\ -45^\circ\ 0^\circ)_4(+45^\circ\ -45^\circ)]$-lay-up. Two specimen geometries are used: a regular cruciform specimen and a cruciform specimen into which a central hole is drilled. The latter is made in order to enhance the already heterogeneous deformation field. The method is based on a finite element calculated strain field of a cruciform specimen loaded in both orthogonal axes and the measured strain field obtained by digital image correlation. The obtained material parameters agree reasonably well with the values obtained by traditional uniaxial tensile tests. However, the results based on the regular cruciform specimen without a hole, show less variance than the results obtained with the perforated specimen. This is possibly due to the fact that the digital image correlation technique has some difficulties measuring steep deformation gradients, hence inducing errors in the measurement of the displacement and strain maps. Further investigation is needed to clarify this inconvenience. The objective of the experiment is to enforce a material behaviour that exposes the different elastic material parameters. If this is achieved by a non-perforated specimen, there is no need for a more complex geometry that could possibly lead to further measurement errors.

ACKNOWLEDGEMENTS

This project is supported by the Belgian Science Policy through the IAP P05/08 project and the European Commission in the framework of the specific research

and technology development program Energy, Environment, and Sustainable Development with contract number ENK6-CT-2001-00552. The authors also express their gratitude to Hans Tommerup Knudsen from LM Glassfiber in Denmark for his efforts in producing the cruciform specimens.

REFERENCES

1 **Lin, W. P.** and **Hu, H. T.** Parametric study of failure stresses in fibre reinforced composite laminates subjected to biaxial tensile load. *J. Compos. Mater.*, 2002, **36**(12), 1481–1504.

2 **Hinton, M. J., Kaddour, A. S.,** and **Soden, P. D.** *Failure criteria in fibre reinforced polymer composites: the world-wide failure exercise*, 2004 (Elsevier).

3 **Boehler, J. P., Demmerle, S.,** and **Koss, S.** A new direct biaxial testing machine for anisotropic materials. *Expl. Mech.*, 1994, **34**(1), 1–9.

4 **Soden, P. D., Hinton, M. J.,** and **Kaddour, A. S.** Biaxial test results for strength and deformation of a range of E-glass and carbon fibre reinforced composite laminates: failure exercise benchmark data, *Compos. Sci. Technol.*, 2002, **62**(12), 1489–1514.

5 **Welsh, J. S.** and **Adams, D. F.** Development of an electromechanical triaxial test facility for composite materials. *Expl. Mech.*, 2000, **40**(2), 312–320.

6 **Zouani, A., Bui-Quoc, T.,** and **Bernard, M.** A proposed device for biaxial tensile fatigue testing. *Fatig. Fract., ASME PVP-323*, 1996, **1**, 331–339.

7 **Swanson, S. R., Christoforou, A. P.,** and **Colvin, G. E.** Biaxial testing of fiber composites using tubular specimens. *Expl. Mech.*, 1988, **28**(2), 238–243.

8 **Pascoe, K. J.** and **de Villers, J. W. R.** Low cycle fatigue of steels under biaxial straining. *J. Strain Analysis*, 1967, **2**(2), 117–126.

9 **Parsons, M. W.** and **Pascoe, K. J.** Development of a biaxial fatigue testing rig. *J. Strain Analysis*, 1975, **10**, 1–9.

10 **Smits, A., Van Hemelrijck, D., Philippidis, T. P.,** and **Cardon, A.** Design of a cruciform specimen for biaxial testing of fibre reinforced composite laminates. *Compos. Sci. Technol.*, 2006, **66**(7–8), 964–975.

11 **Yu, Y., Wan, M., Wu, X. D.,** and **Zhou, X. B.** Design of a cruciform biaxial tensile specimen for limit strain analysis by FEM. *J. Mater. Process. Technol.*, 2002, **123**(1), 67–70.

12 **Mayes, J. S., Welsh, J. S.,** and **Key, C. T.** Biaxial failure envelope for a glass fabric reinforced composite laminate. Final report PO N00167-01-M-0246, Mayes Consulting Engineers, 2002, pp. 1–13.

13 **Welsh, J. S.** and **Adams, D. F.** An experimental investigation of the biaxial strength of IM6/3501-6 carbon/epoxy cross ply laminates using cruciform specimens. *Compos. A, Appl. Sci.*, 2002, **33**(6), 829–839.

14 **Lecompte, D., Smits, A., Sol, H., Vantomme, J.,** and **Van Hemelrijck, D.** Mixed numerical-experimental technique for orthotropic parameter identification using biaxial tensile tests on cruciform specimens. *Int. J. Solids Struct.*, 2007, **44**(5), 1628–1642.

15 **Lecompte, D.** *Elastic and elasto-plastic material parameter identification by inverse modeling of static tests using digital image correlation*. PhD Thesis, Free University of Brussels (VUB), 1 220, 2007.

16 **Bui, H. D.** *Inverse problems in the mechanics of materials: an introduction*, 1994, pp. 1–224 (CRC Press Inc., Florida).

17 **Van Hemelrijck, D.** *Reliable optimal use of materials for wind turbine rotor blades (OPTIMAT blades)*, contract no. ENK6-CT-2001-00552, project no. NNE5-2001-00174.

18 **Dawicke, D. S.** and **Pollock, W. D.** Biaxial testing of 2219-T87 aluminum alloy using cruciform specimens. NASA contractor report 4782, Langley Research Centre, Hampton, Virginia, 1997.

APPENDIX

Notation

$\Delta \boldsymbol{p}$	column vector of the parameter updates of E_1, E_2, G_{12}, and ν_{12}
$\boldsymbol{\varepsilon}^{\exp}$	column vector of the experimental strains
$\boldsymbol{\varepsilon}^{\text{num}}(\boldsymbol{p}^k)$	column vector of the finite element strains as a function of the four parameters at iteration k
$\mathbf{S}^t$	sensitivity matrix

JAERO199

Queries

D V Hemelrijck, A Makris, C Ramault, E Lamkanfi, W V Paepegem, and D Lecompte

In IMechE journals, the style given below is followed for vector and matrix notations: **Matrices** bold roman and ***vectors*** bold italic. Please confirm whether we have correctly identified all these notations in the article.

In the manuscript, terms like "p" and "S" in equations were set with underline and double underline, respectively. We have removed those underlines, and have set them as per journal style. Please check and confirm.

Q1 There is a discrepancy in the subscripts "4" and "3" given for "$[(+45^\circ\ 45^\circ\ 0^\circ)_4(+45^\circ\ 45^\circ)]$" and "$[(+45^\circ\ 45^\circ\ 0^\circ)_3(+45^\circ\ -45^\circ)]$". Please check.

Q2 Please check and advise the organization name in acknowledgement is correct or not.

Q3 Please provide publisher's location in reference [2].

Q4 Please check "1 220" given in reference [15].